RSC Advances

PAPER

View Article Online
View Journal | View Issue

Cite this: *RSC Adv.*, 2020, **10**, 20057

Spectroscopic analysis of Eu^{3+} doped silica–titania–polydimethylsiloxane hybrid ORMOSILs†

Manju Gopinath R. J., Subash Gopi, Sanu Mathew Simon, A. C. Saritha, P. R. Biju, Cyriac Joseph and N. V. Unnikrishnan *

Received 5th April 2020
Accepted 17th May 2020

DOI: 10.1039/d0ra03073b

rsc.li/rsc-advances

Eu^{3+} doped silica–titania–polydimethylsiloxane hybrid ORMOSILs were synthesized *via* a non-hydrolytic sol–gel route. The structural and thermal analyses of the samples confirmed that the matrix structure remains unaffected by doping with different concentrations of Eu^{3+} ions. Photoluminescence (PL) studies performed at 394 nm on Eu^{3+} doped ORMOSILs imply that they emit broad blue host emission and the characteristic Eu^{3+} red emissions simultaneously. Also, the samples were excited at the charge transfer (CT) band and this confirmed the existence of an energy transfer path from the host to the Eu^{3+} ions *via* Ti^{4+}–O^{2-}–Eu^{3+} bonds. The phonon energy of the host matrix was estimated by phonon sideband (PSB) analysis and the results were substantiated by Raman analysis. Judd–Ofelt (JO) parameters were also evaluated which give details about the local surroundings of the Eu^{3+} ions in the system and these parameters were further used for predicting the radiative properties of $^5D_0 \rightarrow {}^7F_{1,2,4}$ transitions of Eu^{3+} ions. Furthermore, the quantum efficiency and CIE co-ordinates were evaluated and it was found that Eu^{3+} doped silica–titania–polydimethylsiloxane ORMOSIL has an intense pinkish red emission with a quantum efficiency of 30.7%.

1. Introduction

Research has been progressing for decades on the development of luminescent materials and their applications in fabricating optical devices. Materials doped with rare-earths (REs) have drawn considerable attention due to their excellent fluorescent properties. Cerium, samarium, europium, gadolinium, terbium, dysprosium, erbium, and ytterbium are some of the rare-earths commonly used for luminescence applications. But the intensity of emission by these rare-earths is greatly influenced by the site and its neighbourhood occupied by the RE ions in the host matrix.[1] Europium (Eu^{3+}) ions emit radiation in the red region resulting from the $^5D_0 \rightarrow {}^7F_2$ hypersensitive transition and its intensity is highly influenced by the symmetry of the positions occupied by Eu^{3+} ions in the host matrix. Consequently, the Eu^{3+} ions are effectively used to explore the symmetry and bonding nature around these dopant ions in the system.[2] Hence new host matrices are developed to incorporate these RE ions and the study of the performance of the RE ions in these new systems is a fascinating field of research in material science. Thus a new family of organically modified silicate is introduced as host matrix in the present work.

The electrons that are excited to the $^5D_{1,2,3}$ levels of the Eu^{3+} ions de-excites non-radiatively to the $^5D_0$ level by multiphonon relaxation. Studies show that the multiphonon decay rate increases with increase in phonon energy and electron–phonon coupling strength.[3,4] Hence it is also important to estimate the phonon energy associated with the present glass system.

In many recent works, silica is effectively used as the host matrix to incorporate the rare-earth ions so that these ions can be protected from the environmental effects and can enhance emission intensity.[5] Also, the binary matrices such as TiO_2–SiO_2 and TiO_2–ZrO_2 doped with RE ions were widely examined during the last decades as they find applications in lasers, lighting and displays, up-conversion and white light emission.[6–9] However, the surface defects and lattice distortions in these host matrices adversely influence the luminescence properties of the RE ions which leads to quenching of luminescence.[4] Hence the decay life time and luminescence intensity of these host matrices have to be improved. To achieve this goal, organics are incorporated into the inorganic matrix which leads to the formation of new Organically Modified Silicates (ORMOSILs) and Organically Modified Ceramers (ORMOCERs) with improved mechanical, thermal and optical properties.[10] In the light of the above investigations, the present work aims at the preparation and characterisation of polydimethylsiloxane modified silica–titania (SiO_2–TiO_2–PDMS) ORMOSIL matrix doped with Eu^{3+} ions. Here, PDMS is selected as the organic polymer for modifying the silica–titania inorganic matrix because both PDMS and SiO_2 have similar –Si–O–Si– chemical

School of Pure and Applied Physics, Mahatma Gandhi University, Kottayam, Kerala, 686560, India. E-mail: nvu100@yahoo.com

† Electronic supplementary information (ESI) available. See DOI: 10.1039/d0ra03073b

bond and hence forms covalently bonded network.[11,12] Here non-hydrolytic route of sol–gel method is adopted for the sample preparation since the organic polymer PDMS is insoluble in water and TiO_2 precipitates in the hydrolytic process.[13]

Interestingly, the silica–titania–polydimethylsiloxane (SiO_2–TiO_2–PDMS) host matrix has a broad blue emission peaking at 470 nm when excited with UV light.[14] Thus the photoluminescence emission of the Eu^{3+} doped SiO_2–TiO_2–PDMS hybrid matrix is the resultant of the blue emission of the host matrix and the red emission of the Eu^{3+} ions which finds application in WLEDs, novel luminescent phosphors, displays *etc.*

2. Experimental details

The inorganic precursors for synthesising the samples were tetraethyl orthosilicate/TEOS (Merck) and titanium(IV) isopropoxide/TIP (Aldrich) which contains SiO_2 and TiO_2 respectively. The organic polymer for modifying the inorganic was OH-terminated polydimethylsiloxane/PDMS (MW = 4200) (Alfa Aesar). Here, ethanol (Merck) was the solvent and hydrochloric acid (HCl) was the catalyst. The source of Eu^{3+} ions for doping was europium(III) nitrate hexahydrate (Alfa Aesar). The molar ratio of (SiO_2 + PDMS)/TiO_2 is taken as 3 : 1. The SiO_2 and PDMS were taken together since the organic polymer PDMS has the same –Si–O–Si– bonding as that of SiO_2.

Mixtures 1 and 2 were prepared during synthesis. Mixture 1 contains 5.2 mL of TEOS, 0.1 mL of PDMS and 5.8 mL of ethanol and the molar ratio of EtOH/TEOS is kept as 4. Mixture 2 consists of 1.9 mL of TIP and 1.8 mL of ethanol where the molar ratio of EtOH/TIP is kept as 5. After stirring these mixtures separately for 30 minutes, they were added together and the stirring was further continued for another one hour. Europium(III) nitrate hexahydrate dissolved in ethanol was then added to the resultant SiO_2–TiO_2–PDMS mixture in various concentrations ranging from 1 to 4 wt% and hydrochloric acid was also added in very small quantity. This mixture is vigorously stirred to obtain a clear and homogenous sol which is transferred to polypropylene petridish and covered with para film. These dishes were kept without any disturbance until transparent glass samples were formed. All the synthesis procedures were carried out at room temperature and normal atmospheric conditions. In this discussion undoped ORMOSIL host matrix SiO_2–TiO_2–PDMS is denoted as Eu0 and the Eu^{3+} doped samples were denoted as Eu1, Eu2, Eu3 and Eu4 for 1, 2, 3 and 4 wt% doping respectively.

X-Ray powder diffraction analysis and Fourier transform infra-red characterization were carried out for the analysis of the sample structure using PANalytical X'Pert PRO and Perkin Elmer Spectrum 400 respectively. The thermal stability of the samples was studied using PerkinElmer STA 8000 thermo gravimetric analyser. Also, Flurolog-3 Spectrofluorometer (Horiba Scientific) was used for photoluminescence characterisations and Fluoromax-4, TCSPC Fluorescence Lifetime Measurement System (Horiba Scientific) for lifetime measurements. The Raman spectra of the samples were also recorded for analysing the phonon side band (PSB) using WITec Alpha 300 RA Confocal Raman Spectrometer.

3. Results and discussions

3.1 XRD analysis

X-Ray diffraction analyses were carried out on the pure host matrix Eu0 and samples doped with varying Eu^{3+} concentrations. All the samples show identical diffraction pattern and hence the patterns of representative samples Eu0, Eu2 and Eu4 are depicted in Fig. S1.† The X-ray diffraction pattern has a broad hump between 15° and 30° which is a characteristic of the SiO_2 component of the host matrix.[15,16] Here, the peaks of TiO_2 are not distinctly visible as the amorphous nature of SiO_2 is prominent. The diffraction patterns of all the samples also show similar behaviour which confirms that the structure of the host matrix remains unaltered even after Eu^{3+} doping.

3.2 FTIR analysis

The FTIR spectroscopy can be adopted as an effective tool for analysing the chemical and structural changes of the host matrix with Eu^{3+} doping. The FTIR spectra of the pure (Eu0) and Eu^{3+} doped samples (Eu2 and Eu4) were recorded from 400 cm^{-1} to 4000 cm^{-1} and are shown in Fig. 1.

The FTIR spectra of pure and Eu^{3+} doped samples show identical nature in respect of peak positions and intensity. The small peak at 849 cm^{-1} in the spectra establishes that copolymerisation reaction has occurred between Si–OH groups of hydrolysed TEOS and PDMS molecules. Also, the peak located at 945 cm^{-1} is ascribed to the Si–O–Ti bond formed during condensation reaction. The asymmetric vibration of Si–O–Si bonds results in the absorption band at 1066 cm^{-1}.[17] Also, the band at 803 cm^{-1} is assigned to the net effect of Si–C stretching and CH_3 rocking in Si–CH_3 and that at 1267 cm^{-1} is due to the symmetric deformation of CH_3 in Si–CH_3 group.[18,19] Mackenzie *et al.* have suggested in the report on SiO_2–PDMS ORMOSIL that the –CH_3 groups in Si–CH_3 performs in a way similar to the non-bonding oxygen in silicate glasses.[20] Thus it can be concluded

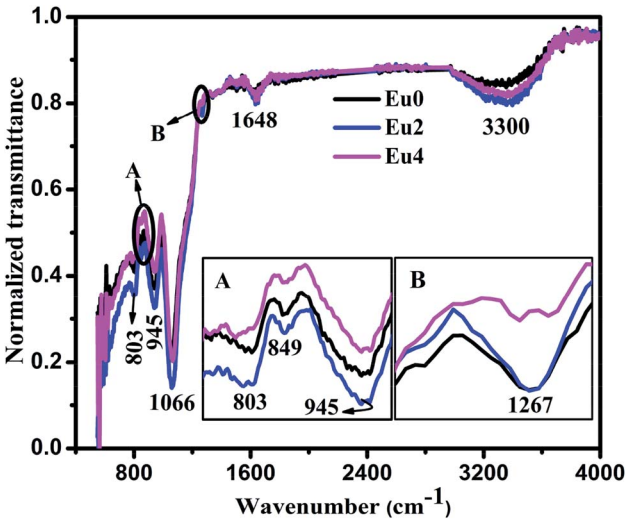

Fig. 1 FTIR spectra of pure and Eu^{3+} doped SiO_2–TiO_2–PDMS ORMOSIL samples (inset figures (A and B) shows the peaks in the range 750 cm^{-1} to 975 cm^{-1} and 1240 cm^{-1} to 1275 cm^{-1} respectively).

that the FTIR spectroscopy confirms the presence of oxygen related defects in the host matrix which plays an important role in the luminescence properties of the SiO_2–TiO_2–PDMS ORMOSIL host matrix.[14] Absorption bands were also present at 1648 cm^{-1} and 3300 cm^{-1} which occurs by the stretching and bending vibrations of surface adsorbed water and OH groups respectively.[21] The similarity in the FTIR spectra of both pure and Eu^{3+} doped samples further confirms that the matrix structure remains unchanged by doping with different concentrations of Eu^{3+} ions.

3.3 TG analysis

Thermo gravimetric (TG) analysis was done in the nitrogen atmosphere up to 700 °C to study the thermal stability of pure and Eu^{3+} doped samples and the curves are illustrated in Fig. S2.†

The TG curves depicts that a weight loss of only 15% occurred on heating up to 150 °C for all the samples. This is due to the evaporation of adsorbed water and trapped solvents in the matrix, whose presence is confirmed in FTIR analysis.[21] The curves become almost straight in the range 150–700 °C and is indicating that the samples are thermally stable up to 700 °C. The similar nature of TG curves for the pure and doped samples confirms that the matrix structure remains unaffected by Eu^{3+} doping.

3.4 Photoluminescence analysis

The photoluminescence (PL) analysis is used as an efficient tool for investigating the energy level transitions in Eu^{3+} doped SiO_2–TiO_2–PDMS ORMOSILs. The excitation spectra of the samples were recorded fixing λ_{em} at 613 nm which is the prominent emission wavelength of Eu^{3+} ions. The excitation spectra of all the samples are depicted in Fig. S3† and as a representative case, the spectrum of 2 wt% Eu^{3+} doped SiO_2–TiO_2–PDMS ORMOSIL (Eu2) is shown in Fig. 2.

The excitation spectrum of Eu2 sample consists of a broad band peaking at 276 nm which is due to the overlapping of the O–Eu charge transfer (CT) band and the SiO^-–Ti ligand-to-metal electron transfer [LMET] band. This indicates an energy transfer from the O–Ti charge transfer band to the Eu^{3+} ions in the SiO_2–TiO_2–PDMS system.[22,23] The lines at 360, 374, 380, 394, 414, 464 and 524 nm are assigned to the electronic transitions of Eu^{3+} ions from the ground $^7F_0$ level to $^5D_4$, $^5G_4$, $^5G_2$, $^5L_6$, $^5D_3$, $^5D_2$ and $^5D_1$ levels respectively. Also, there is a peak at 534 nm which corresponds to the $^7F_1 \rightarrow {}^5D_1$ energy level transition of Eu^{3+} ions.[2] The peak at 450 nm is the phonon sideband of the host matrix which will be discussed in the forthcoming section. The prominent excitation transition at 394 nm and the charge transfer band were chosen for the investigation of the photoluminescence characteristics of Eu^{3+} doped SiO_2–TiO_2–PDMS ORMOSILs.

The emission spectra of all the samples were obtained upon excitation at 394 nm and are shown in Fig. 3. Here, the spectra consist of a broad emission peaking at 450 nm which is assigned to the oxygen related defects in the host matrix.[21,24] The authors reported in their previous work that the pure SiO_2–TiO_2–PDMS host matrix has a weak excitation around 276 nm and a strong excitation around 396 nm, monitoring the emission at 470 nm.[14] Hence, when the Eu^{3+} doped system is excited at 394 nm, both the host matrix and the Eu^{3+} ions were excited giving host emission along with the characteristic emissions of Eu^{3+} ions as shown in the spectra. It is observed that the host emission intensity increases with increase in Eu^{3+} doping concentration. As the Eu^{3+} ions were embedded in the host matrix, its lattice gets distorted due to the difference in the radius of Eu^{3+} ions (0.098 nm) and Ti^{4+} ions (0.061 nm). Also, a charge imbalance exists between Eu^{3+} and Ti^{4+} ions which leads to the formation of oxygen vacancies.[6,25] Thus as the Eu^{3+}

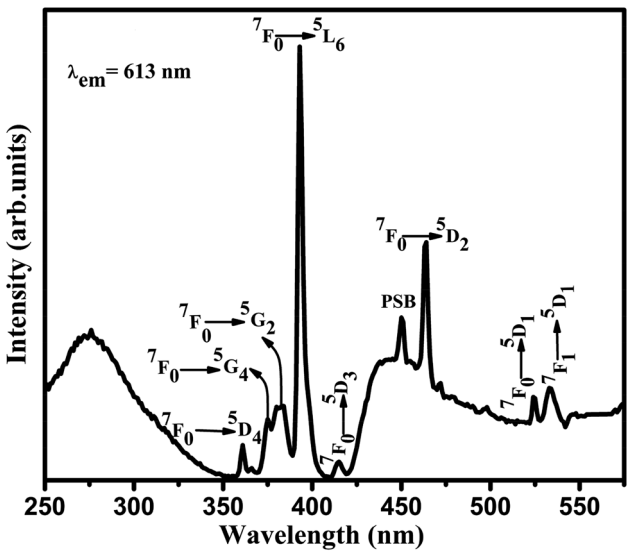

Fig. 2 Excitation spectrum of 2 wt% Eu^{3+} doped SiO_2–TiO_2–PDMS ORMOSIL sample.

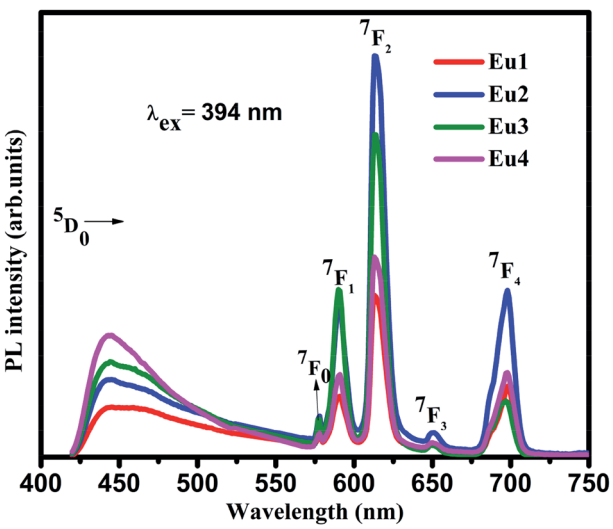

Fig. 3 Emission spectra of Eu^{3+} doped SiO_2–TiO_2–PDMS ORMOSILs excited at 394 nm.

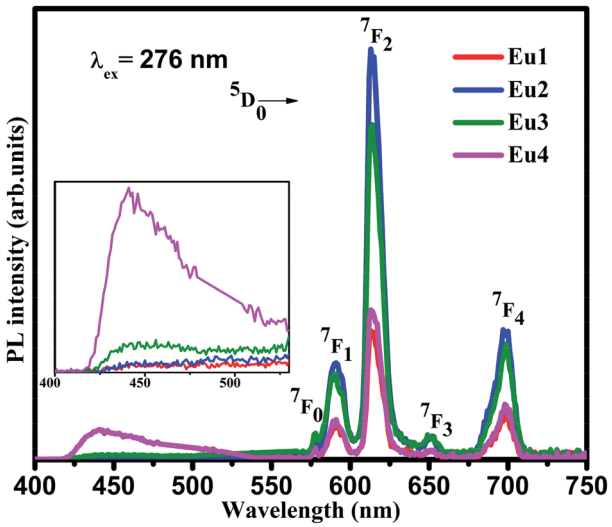

Fig. 4 Emission spectra of Eu^{3+} doped SiO_2–TiO_2–PDMS ORMOSILs excited at 276 nm (inset shows the magnified image of the host emission in the range 400–550 nm).

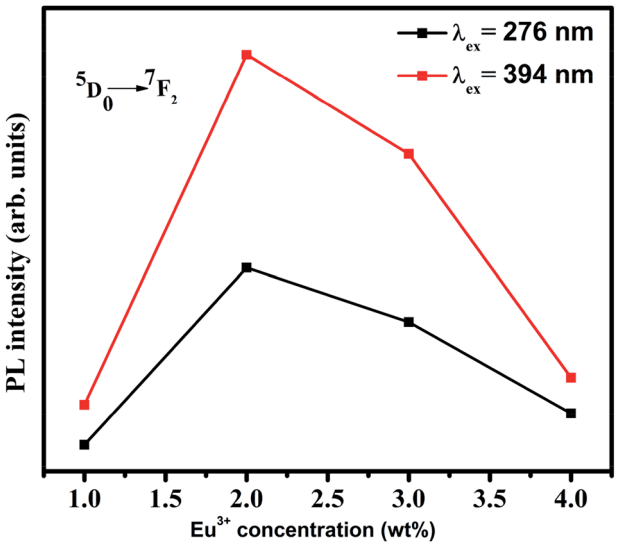

Fig. 5 Variation of PL intensity of 613 nm emission with Eu^{3+} concentration.

ion concentration increases, these defects also increases which in turn enhances the host emission.

The line emissions in the spectra correspond to $^5D_0 \rightarrow {}^7F_0$ (577 nm), $^5D_0 \rightarrow {}^7F_1$ (590 nm), $^5D_0 \rightarrow {}^7F_2$ (613 nm), $^5D_0 \rightarrow {}^7F_3$ (651 nm) and $^5D_0 \rightarrow {}^7F_4$ (698 nm) transitions of Eu^{3+} ions.[2,6] Though the electrons were excited to the higher energy levels of Eu^{3+} ions, only radiative transitions from $^5D_0$ level to the lower f levels were observed in the emission spectra. This indicates the existence of non-radiative transition from the higher energy levels to $^5D_0$ level. Even though $^5D_0 \rightarrow {}^7F_0$ and $^5D_0 \rightarrow {}^7F_3$ transitions are present in the spectra, they are forbidden according to the Judd–Ofelt (JO) theory. The presence of these transitions were due to J-mixing which is enhanced by strong crystal-field effects of the host matrix.[2] Hence it can be confirmed that the Eu^{3+} ions have asymmetric vicinity in the matrix. Furthermore, the $^5D_0 \rightarrow {}^7F_0$ transition is narrow which confirms that the Eu^{3+} ions occupy asymmetric sites in the host matrix which is a characteristic of amorphous hybrid samples.[26]

The $^5D_0 \rightarrow {}^7F_1$ transition is a magnetic dipole transition while the $^5D_0 \rightarrow {}^7F_2$ transition is an electric dipole transition. Hence the $^5D_0 \rightarrow {}^7F_1$ transition does not depend on local environment of the Eu^{3+} ions while the $^5D_0 \rightarrow {}^7F_2$ transition is affected by the local surroundings of the Eu^{3+} ions and the nature of the ligands in the host matrix. Thus the $^5D_0 \rightarrow {}^7F_2$ transition is a hypersensitive transition which can be used as a probe to measure the asymmetry of Eu^{3+} occupied site. On exciting the samples at 394 nm, the peak corresponding to $^5D_0 \rightarrow {}^7F_2$ transition at 613 nm is very strong compared to $^5D_0 \rightarrow {}^7F_1$ transition at 590 nm. As the Eu^{3+} ions occupy asymmetric sites in the host matrix the electric dipole transition dominates the magnetic dipole transition.[27] Hence it can be concluded from the photoluminescence studies that the Eu^{3+} ions occupy asymmetric sites in the SiO_2–TiO_2–PDMS ORMOSIL host matrix. The luminescence intensity is found to increase with an increase in the Eu^{3+} ion concentration up to 2 wt%. The glass exhibits luminescence quenching above this concentration and hence 2 wt% Eu^{3+} is the optimum doping concentration in the present system. As the number of Eu^{3+} activator ions increase, the interionic distance decreases which results in a fast energy transfer between the ions. Thus a part of the excitation energy is non-radiatively dissipated resulting in the quenching of luminescence.[28]

The emission spectra were also recorded on exciting the Eu^{3+} doped samples in the CT band (276 nm) and are shown in Fig. 4. The spectra shows similar nature as that of the directly excited samples which clarifies that the Eu^{3+} ions in the same site are excited in both cases. The Eu^{3+} activator ions are not directly excited in the CT band but the high emission intensity of the Eu^{3+} ions may be due to the efficient energy transfer from the host matrix to the Eu^{3+} activator ions *via* Ti^{4+}–O^{2-}–Eu^{3+} bond.[29]

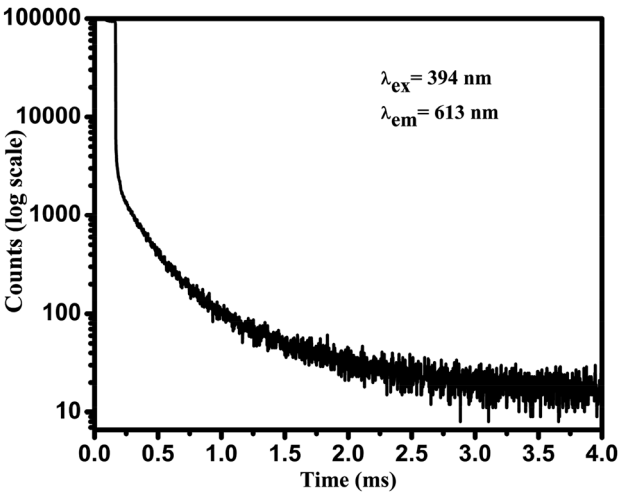

Fig. 6 Luminescence decay time profile of 2 wt% Eu^{3+} doped SiO_2–TiO_2–PDMS ORMOSIL sample.

Table 1 Comparison of average life time of Eu^{3+} ions in similar host matrices

Sample	Average lifetime, τ (ms)	Reference
SiO_2–TiO_2–PDMS–Eu^{3+}	0.900	Present work
EuTTA–PMMA	0.364	32
TPBFEu16	1.2002	3
SiO_2–PMMA–Eu^{3+}	0.275	26
TiO_2–Eu^{3+}	0.550	33

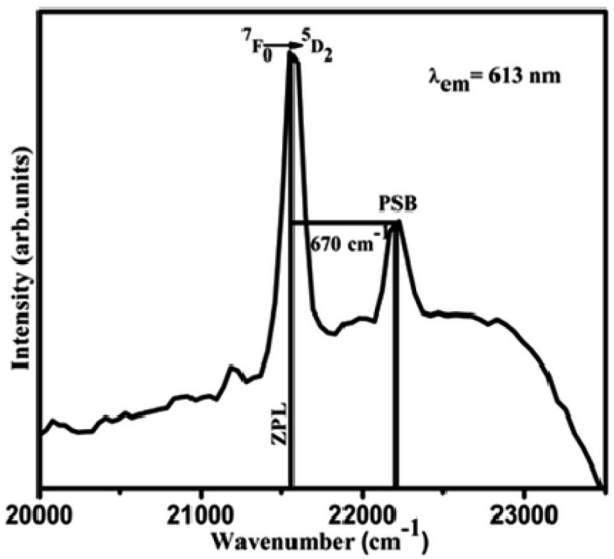

Fig. 7 Phonon sideband spectrum of 2 wt% Eu^{3+} doped SiO_2–TiO_2–PDMS ORMOSIL with $^7F_0 \rightarrow {}^5D_2$ excited state transition.

When the samples are excited at 276 nm, the electrons in the O 2p states are excited to the Ti 3d states of the host matrix which is transferred to the 4f state of the Eu^{3+} ions.[25] Thus the Eu^{3+} activator ions are efficiently sensitized by the host. Since the excited electrons in the host matrix are transferred to the Eu^{3+} ions, the host emission intensity is not prominent in the spectra. The magnified image in the inset of Fig. 4 shows that though the host emission intensity is feeble, the trend shown is same as that of the directly excited samples. This confirms that the Eu^{3+} insertion in to the host matrix generates defects which in turn increases the host emission. The variation in the photoluminescence intensity of $^5D_0 \rightarrow {}^7F_2$ transition with Eu^{3+} concentration in both the excitation wavelengths are also depicted in Fig. 5.

The luminescence life time of 2 wt% Eu^{3+} doped SiO_2–TiO_2–PDMS ORMOSIL (Eu2) was evaluated by monitoring the decay profile of 613 nm emission of the sample on exciting with 394 nm and the luminescence time spectrum is shown in Fig. 6.

The average fluorescence lifetime (τ) of the energy level can be obtained from the formula, $\tau = \frac{\int tI(t)\mathrm{d}t}{\int I(t)\mathrm{d}t}$, where $I(t)$ represents the luminescence intensity at time t.[30] The average lifetime of Eu2 ORMOSIL glass was found to be 0.90 ms. A relatively longer lifetime of the sample shows that the Eu^{3+} ions are evenly embedded in the host matrix so that ion clustering is reduced.[29] The nature of the decay curve also indicates that the Eu^{3+} ions are present in an asymmetric environment in the host matrix.[31] A comparative study with the lifetimes of other Eu^{3+} doped samples are tabulated in Table 1.

The asymmetric ratio (R) is another effective tool to analyse the symmetry of site occupied by Eu^{3+} ions in the host matrix. It is the ratio between the integrated emission intensity of $^5D_0 \rightarrow {}^7F_2$ and $^5D_0 \rightarrow {}^7F_1$ energy level transitions.[6] As discussed earlier, $^5D_0 \rightarrow {}^7F_2$ transition is due to the electric dipole mechanism and $^5D_0 \rightarrow {}^7F_1$ transition due to magnetic dipole mechanism which is not affected by the local surroundings of the ions. Hence the intensity of $^5D_0 \rightarrow {}^7F_1$ transition is taken as the reference. Thus the R values can be used to understand the asymmetry in the neighbourhood of Eu^{3+} ions in the host matrix and also the degree of covalency between Eu^{3+} and O^{2-} ions.[1,3] The R values obtained in the present study are 3.35, 3.44, 3.37 and 2.5 for Eu1, Eu2, Eu3 and Eu4 samples respectively. The larger values of R indicates that the asymmetry and covalency effect around the Eu^{3+} ion site is higher in the present system. Julian *et al.* have reported that the R value is in between 3 and 6 for Eu^{3+} doped silica glasses, polymers or crystals.[34] Also as the Eu^{3+} ion concentration increases, the R value reaches a maximum for Eu2 sample and decreases above that concentration. This confirms the cluster forming tendency of Eu^{3+} ions at higher concentration which leads to luminescence quenching.[35]

3.5 Phonon sideband analysis

The Eu^{3+} ions doped in the SiO_2–TiO_2–PDMS host matrix are excited to $^5D_{1,2,3,4}$, $^5L_6$, $^5G_2$ energy levels. But the phonon energy of the sample hinders the radiative emission from these higher energy levels to the ground state. Hence, all these excited

Table 2 Phonon energy ($\hbar\omega$), electron-phonon coupling constant and non-radiative decay rate for the $^5D_1$, $^5D_2$ and $^5D_3$ levels of the 2 wt% Eu^{3+} doped SiO_2–TiO_2–PDMS ORMOSIL (Eu2)

		$^7F_0 \rightarrow {}^5D_1$		$^7F_0 \rightarrow {}^5D_2$		$^7F_0 \rightarrow {}^5D_3$	
$\hbar\omega$ (cm^{-1})	g	α ($\times 10^{-3}$ cm)	W_{mp}/W_0	α ($\times 10^{-3}$ cm)	W_{mp}/W_0	α ($\times 10^{-3}$ cm)	W_{mp}/W_0
670	0.2984	1.667	0.0541	2.169	0.0044	2.35	0.0014

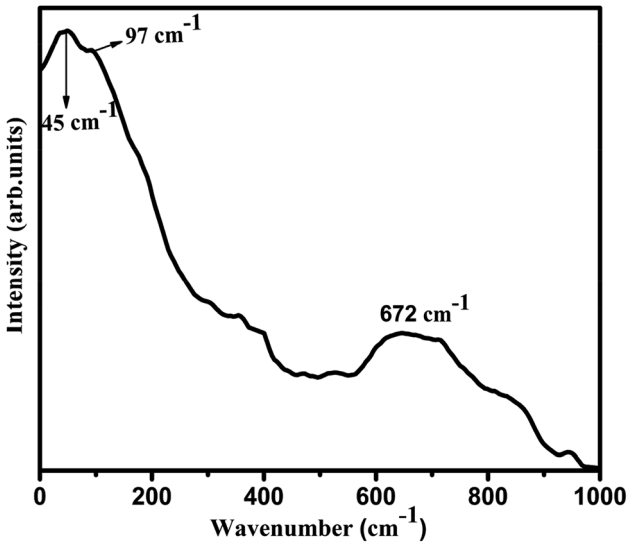

Fig. 8 Raman spectrum of 2 wt% Eu^{3+} doped SiO_2–TiO_2–PDMS ORMOSIL sample.

electrons of Eu^{3+} ions can populate the lowest excited $^5D_0$ energy level after non-radiative decay. From this $^5D_0$ level, the excited electrons return to the ^7F_J ($J = 1, 2, 3, 4$) ground state emitting its characteristic radiation. The excitation spectrum of Eu^{3+} doped SiO_2–TiO_2–PDMS ORMOSIL contains a peak in the higher energy side of the pure electronic band (PEB) transition, $^7F_0 \rightarrow {}^5D_2$ and this peak is assigned as the phonon sideband (PSB) as shown in Fig. 7. The PSB analysis is carried out to study the multiphonon relaxation in Eu^{3+} doped SiO_2–TiO_2–PDMS ORMOSIL host matrix.

The PSB includes simultaneous vibrational and electronic transitions and its presence in the excitation spectrum is an indication of the coupling of excited electrons with the excess energy of vibrational modes around the Eu^{3+} ions. The difference in energy between the PEB and PSB band corresponds to the phonon energy, $\hbar\omega$ and here it is estimated to be 670 cm^{-1}. The coupling of a particular vibrational mode to an electronic transition is termed as electron-phonon coupling strength, g and is estimated to be 0.2984 for Eu^{3+} doped SiO_2–TiO_2–PDMS ORMOSIL. Similar high values of g was also reported for Eu^{3+} doped ZrO_2–PEG composites[35] and for Eu^{3+} doped SiO_2–TiO_2–ZrO_2 glasses.[4] Also, L. Skuja has reported the significance of electron-phonon coupling constant (g) in optical transition. That is if the g value is below ~4, the optical absorption or luminescence spectra contains zero-phonon and vibronic lines even at low temperatures.[36] The relative non-radiative decay rate

Table 4 Comparison of JO intensity parameters of 2 wt% Eu^{3+} doped SiO_2–TiO_2–PDMS ORMOSIL with other glass hosts

Sample	Ω_2 ($\times 10^{-20}$)	Ω_4 ($\times 10^{-20}$)	Reference
SiO_2–TiO_2–PDMS–Eu^{3+} (Eu2)	6.03	5.18	Present work
SiO_2–PMMA–Eu^{3+}	11.0	—	26
TPBFEu16	3.91	1.54	3
ME17.5	5.32	1.38	4
$U(2000)_{100}$ $Eu(CF_3SO_3)_3$	9.6	8.1	8

W_{mp}/W_0 were also calculated for the $^5D_1$, $^5D_2$ and $^5D_3$ levels of the sample and are tabulated in Table 2. The equations and methods of PSB analysis have been published previously[3,37] and are included in Section S1 of the ESI.†

The observed PSB band for the Eu^{3+} ions in the SiO_2–TiO_2–PDMS ORMOSIL glass is correlated with its Raman spectra which is shown in Fig. 8.

The assignments of chemical bonds in the host matrix that produces the vibrational frequencies in the Raman spectrum are given in Table 3.

Thus it is evident from Raman spectrum that the most energetic vibrational mode which substantially contributes to the appearance of phonon sideband is at 672 cm^{-1} and is correlated with the stretching vibration of Ti–O bond of the host matrix. Furthermore, the presence of Ti–O bond in the Eu2 sample is confirmed in FTIR analysis and also the possibility of charge transfer from Ti–O bond to Eu^{3+} ions is confirmed. Marchese *et al.* have also reported similar photoluminescence emissions in grafted Ti-MCM41 silicas.[41] Thus the features of the phonon side band of Eu2 glass is complementary with its Raman spectrum.

3.6 Judd–Ofelt (JO) analysis

The chemical surroundings of the site occupied by the Eu^{3+} ions in the host matrix has a strong effect on its emission intensity. Judd–Ofelt (JO) theory is a very efficient tool to study the variation in emission intensity of Eu^{3+} ions with its varying chemical environment in the host medium.[4,27] Usually, the JO parameters are determined from the absorption spectrum using the least square fit method. However, in several cases of Eu^{3+} ions, there are difficulties to derive the JO parameters due to (i) thermal corrections[42] (ii) zero magnitude of $U^{(4)}$ matrix element[28] (iii) poor intensity of $^7F_0 \rightarrow {}^5D_2$ level transition.[43] Hence as an alternative method the JO intensity parameters can be calculated from the emission spectrum based on the procedure reported by Peng and Izumitani.[44] The $^5D_0 \rightarrow {}^7F_1$ transition is the magnetic dipole transition and hence its intensity is independent of the host matrix, whereas the $^5D_0 \rightarrow {}^7F_2$, $^5D_0 \rightarrow$

Table 3 Chemical bond assignments of 2 wt% Eu^{3+} doped SiO_2–TiO_2–PDMS ORMOSIL

Vibrational frequency (cm^{-1})			Chemical bond assignments (cm^{-1})	Reference
1	2	Total		
45	97	142	Symmetric stretching vibrations of oxygen atoms in O–Ti–O bond	38
672	—	672	Stretching vibration of Ti–O bond of TiO_6 octahedral units	39 and 40

Table 5 Calculated radiative parameters of 2 wt% Eu^{3+} doped SiO_2–TiO_2–PDMS ORMOSIL[a]

Sl no.	$^5D_0 \rightarrow$	Energy (cm^{-1})	S_{ed} ($\times10^{-22}$)	S_{md} ($\times10^{-22}$)	A_{ed} (s^{-1})	A_{md} (s^{-1})	A (s^{-1})	β_R
1	$^7F_4$	14 463	1.41	0.00	105.74	0.00	105.74	0.3098
2	$^7F_3$	15 433	0.00	0.00	0.00	0.00	0.00	0.0000
3	$^7F_2$	16 283	1.70	0.00	181.37	0.00	181.37	0.5313
4	$^7F_1$	16 943	0.00	0.40	0.00	54.26	54.26	0.1590
5	$^7F_0$	17 320	0.00	0.00	0.00	0.00	0.00	0.0000

[a] Total radiative transition probability, $A_T = 341.37\ s^{-1}$; radiative lifetime, $\tau_R = 2.929$ ms.

Table 6 Comparative study of the quantum efficiency of 2 wt% Eu^{3+} doped SiO_2–TiO_2–PDMS ORMOSIL with similar host matrices

Sample	Quantum efficiency (%)	Reference
SiO_2–TiO_2–PDMS–Eu^{3+} (Eu2)	30.7	Present work
SiO_2–PMMA–Eu^{3+}	18.6	26
SiO_2–TiO_2 (6/4)-Eu^{3+}	9.1	47
SiO_2–TiO_2 (2/8)-Eu^{3+}	8.4	47
TPBFEu16	53.4	3

$^7F_4$ and $^5D_0 \rightarrow {}^7F_6$ transitions are electric dipole transitions and depends upon Ω_2, Ω_4 and Ω_6 values respectively. Among these electric dipole transitions, $^5D_0 \rightarrow {}^7F_6$ transition is weak and falls in the infrared region (~800 nm). Hence this transition is not observed properly due to instrumental limitations. Thus the Ω_6 intensity parameter is taken as zero for determining the radiative parameters of Eu^{3+} ion.[3] The following equation is used for calculating the radiative intensity parameters[45,46]

$$S\left[\frac{^5D_0 \rightarrow {}^7F_{2,4}}{^5D_0 \rightarrow {}^7F_1}\right] = \frac{e^2}{S_{md}}\left(\frac{\nu_J}{\nu_1}\right)^3 \frac{n(n^2+2)^2}{9n^3}\Omega_\lambda \left\langle \psi_J \| U^\lambda \| \psi'_{J'} \right\rangle$$

where ν_1 and ν_J are the wavenumbers in cm^{-1} for the $^5D_0 \rightarrow {}^7F_1$ and $^5D_0 \rightarrow {}^7F_J$ ($J = 2, 4, 6$) transitions respectively. S_{md} gives the magnetic dipole line strength of the $^5D_0 \rightarrow {}^7F_1$ transition of Eu^{3+} ions and n is the refractive index of the glass and for Eu2 glass its value is 1.562. The calculated JO parameters of Eu2 sample are listed in Table 4 and are compared with previous works.

3.7 Radiative parameters

Radiative parameters such as total radiative transition probability (A_T), radiative life time (τ_R) and branching ratios (β_R) for the $^5D_0$ excited state of Eu2 sample have been evaluated from the JO intensity parameters[3,4] and the equations used for calculation are given in Section S2 of the ESI.† The results obtained are tabulated in Table 5. The branching ratio β_R represents the amplification of emission and it is considered that the energy level transition having β_R value greater than 0.50 is good for optical amplification.[3] Here, the transition $^5D_0 \rightarrow {}^7F_2$ (red emission) of the Eu2 sample has relatively high transition probability and branching ratio which confirms that the sample provides good optical amplification to the radiation emitted by the Eu^{3+} ions.

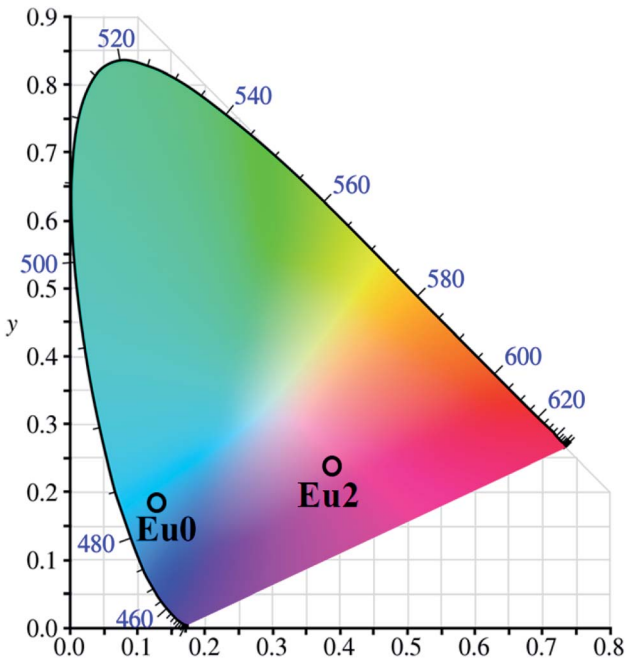

Fig. 9 CIE chromaticity diagram of pure (Eu0) and 2 wt% Eu^{3+} doped SiO_2–TiO_2–PDMS ORMOSIL (Eu2) samples.

Table 7 Effective band width, stimulated emission cross-section, optical gain and experimental branching ratios of the $^5D_0 \rightarrow {}^7F_{1,2,4}$ transitions of 2 wt% Eu^{3+} doped SiO_2–TiO_2–PDMS ORMOSIL sample

Sl no.	$^5D_0 \rightarrow$	$\Delta\lambda_{eff}$ (nm)	σ_e ($\times10^{-22}$) cm^2	Gain-bandwidth ($\times10^{-28}$) cm^3	ΔG ($\times10^{-25}$) cm^2 s	β_{exp}
1	$^7F_4$	13.463	3.190	4.300	9.350	0.3000
2	$^7F_2$	9.450	4.760	4.490	13.929	0.5380
3	$^7F_1$	8.645	1.320	1.140	3.858	0.1610

The experimental lifetime (τ) of Eu2 sample obtained by monitoring the 613 nm emission ($\lambda_{ex} = 394$ nm) is 0.90 ms and the total calculated radiative life time (τ_R) is 2.929 ms. The difference in the lifetimes of the Eu2 sample may be due to the non-radiative decays which is not considered while calculating total radiative lifetime. The ratio between the experimental lifetime and calculated lifetime of the particular excited level gives the luminescence quantum efficiency (η).[2] Thus the quantum efficiency of the Eu2 sample is estimated to be 30.7% with a relative accuracy of 86.7%. The quantum efficiency of the Eu2 sample is also compared with various similar host matrices and are summerized in Table 6.

Also, the effective band-width ($\Delta\lambda_{eff}$), experimental branching ratio (β_{exp}), peak stimulated emission cross-sections (σ_e) and optical gain (ΔG) are estimated from the emission spectrum of Eu2 sample for the $^5D_0 \rightarrow {}^7F_{1,2,4}$ transitions and are represented in Table 7. The branching ratio gives information about the possibility of attaining stimulated emission from any particular transition. Also, the value of the stimulated emission cross-section signifies the gain provided to the emission of the doped rare-earth by the host material. The gain-bandwidth ($\sigma_e \times \Delta\lambda_{eff}$) and optical gain, ΔG ($\sigma_e \times \tau_R$) are also critical parameters which predicts the optical amplification of the host medium in which the rare-earth ions are embedded.[48]

It is clear from Table 7 that the experimental branching ratio agrees well with the calculated values. Among the transitions, $^5D_0 \rightarrow {}^7F_2$ has a relatively higher branching ratio of 53.8% and an emission cross-section of 4.76×10^{-22} cm^2, which proposes that the Eu2 sample can be used for photonic applications. Also, its gain-bandwidth and optical gain values show that the sample can be employed as a good optical amplifier.

3.8 Colorimetric analysis

The color luminescence emission intensities of the samples has been evaluated with Commission International d' Eclairage (CIE) 1931 system and also the dominant emission wavelength of the sample has been identified for evaluating its performance. The CIE co-ordinates calculated are (0.142, 0.192) and (0.411, 0.220) respectively for Eu0 and Eu2 samples and are marked in Fig. 9.

4 Conclusion

XRD, FTIR and TG analyses of Eu^{3+} doped SiO_2–TiO_2–PDMS ORMOSILs confirmed that their structure remain unaltered with Eu^{3+} doping and these samples have appreciable thermal stability. The photoluminescence (PL) analysis by both direct excitation and CT band exhibits similar pattern and SiO_2–TiO_2–PDMS ORMOSIL doped with 2 wt% Eu^{3+} (Eu2) has maximum PL intensity and quenches above that concentration. The JO intensity parameters were determined for Eu2 sample and it was found that $\Omega_2 > \Omega_4$ which is an indication of the asymmetry in sites occupied by the Eu^{3+} ions in the host matrix. The phonon energy ($\hbar\omega$) associated with the non-radiative decay of the host matrix, obtained by Raman analysis (672 cm^{-1}) agrees well with that determined by PSB analysis (670 cm^{-1}). The radiative parameters of $^5D_0 \rightarrow {}^7F_{1,2,4}$ transitions of the Eu2 sample were predicted using JO intensity parameters and the values imply that the Eu2 sample can be used for optical amplification applications. The decay lifetime of the Eu2 sample has been obtained as 0.9 ms which is fairly greater than that of various similar host matrices. The resultant pinkish red emission of the sample having a quantum efficiency of 30.7% confirmed that it can be effectively used in the WLED (RGB) fabrication.

Conflicts of interest

There are no conflicts to declare.

Acknowledgements

The authors are thankful to the University Grants Commission, Govt. of India and to the Department of Science and Technology, Govt. of India for the support in establishing experimental facilities at the School of Pure and Applied Physics, Mahatma Gandhi University, Kottayam, India through SAP-DRS programme No. F.530/12/DRS/2009 (SAP-1) and DST-PURSE programme No.SR/417&418/2017 respectively.

References

1 S. K. Gupta, M. Sahu, K. Krishnan, M. K. Saxena, V. Natarajan and S. V. Godbole, Bluish White Emitting Sr_2CeO_4 and Red Emitting Sr_2CeO_4:Eu^{3+} Nanoparticles: Optimization of Synthesis Parameters, Characterization, Energy Transfer and Photoluminescence, *J. Mater. Chem. C*, 2013, **1**(42), 7054–7063.

2 K. Binnemans, Interpretation of europium(III) spectra, *Coord. Chem. Rev.*, 2015, **295**, 1–45, DOI: 10.1016/j.ccr.2015.02.015.

3 M. S. Sajna, S. Gopi, V. P. Prakashan, M. S. Sanu, C. Joseph, P. R. Biju, *et al.*, Spectroscopic Investigations and Phonon Side Band Analysis of Eu^{3+}-Doped Multicomponent Tellurite Glasses, *Opt. Mater.*, 2017, **70**, 31–40, DOI: 10.1016/j.optmat.2017.04.064.

4 V. P. Prakashan, M. S. Sajna, G. Gejo, M. S. Sanu, P. R. Biju, J. Cyriac, *et al.*, Perceiving Impressive Optical Properties of Ternary SiO_2–TiO_2–ZrO_2:Eu^{3+} Sol–Gel Glasses with High Reluctance for Concentration Quenching: An Experimental Approach, *J. Non-Cryst. Solids*, 2018, **482**, 116–125.

5 J. Reyes, D. Y. Medina, M. Aguilar, M. A. Barron, E. Garfias and A. d. J. Morales, Red, White and Blue Light Emission from Europium Doped Al_2O_3 Confined into a Silica Matrix, *Open J. Appl. Sci.*, 2018, **08**(08), 338–345.

6 M. Chang, Y. Song, Y. Sheng, J. Chen and H. Zou, Understanding the Remarkable Luminescence Enhancement: Via SiO_2 Coating on TiO_2:Eu^{3+} Nanofibers, *Phys. Chem. Chem. Phys.*, 2017, **19**(26), 17063–17074.

7 B. Julián, R. Corberán, E. Cordoncillo, P. Escribano, B. Viana and C. Sanchez, Synthesis and Optical Properties of Eu^{3+}-Doped Inorganic–Organic Hybrid Materials Based on Siloxane Networks, *J. Mater. Chem.*, 2004, **14**(22), 3337–3343.

8 L. D. Carlos, Y. Messaddeq, H. F. Brito, R. A. Sá Ferreira, V. De Zea Bermudez and S. J. L. Ribeiro, Full-Color Phosphors from Europium(III)-Based Organosilicates, *Adv. Mater.*, 2000, **12**(8), 594–598.

9 F. Del Monte, P. Cheben, C. P. Grover and J. D. Mackenzie, Preparation and Optical Characterization of Thick-Film Zirconia and Titania Ormosils, *J. Sol-Gel Sci. Technol.*, 1999, **15**(1), 73–85.

10 H. Schmidt and W. Herbert, Organically Modified Ceramics And Their Applications, *J. Non-Cryst. Solids*, 1990, **121**, 428–435.

11 K. Chakrabarti and C. M. Whang, Silver Doped ORMOSIL – An Investigation on Structural and Physical Properties, *Mater. Sci. Eng., B*, 2002, **88**(1), 26–34.

12 J. Wen and G. L. Wilkes, Organic/Inorganic Hybrid Network Materials by the Sol–Gel Approach, *Chem. Mater.*, 1996, **8**(8), 1667–1681.

13 J. N. Hay and H. M. Raval, Synthesis of Organic–Inorganic Hybrids via the Non-hydrolytic Sol–Gel Process, *Chem. Mater.*, 2001, **13**, 3396–3403.

14 R. J. M. Gopinath, V. Vidyadharan, S. M. Simon, A. C. Saritha, P. R. Biju, C. Joseph, *et al.*, Investigations on the Blue Luminescence Enhancement of Organically Modified SiO_2–TiO_2–PDMS Glass Matrix, *Nano-Struct. Nano-Objects*, 2019, **20**, 100377, available from: https://linkinghub.elsevier.com/retrieve/pii/S2352507X19302999.

15 V. Vidyadharan, P. Vasudevan, S. Karthika, C. Joseph, N. V. Unnikrishnan and P. R. Biju, Structural , Optical and AC Electrical Properties of Ce^{3+}-Doped TiO_2–SiO_2 Matrices, *J. Electron. Mater.*, 2015, **44**(8), 2754–2761.

16 M. Shwetha and B. Eraiah, Influence of Europium (Eu^{3+}) Ions on the Optical Properties of Lithium Zinc Phosphate Glasses, *IOP Conf. Ser.: Mater. Sci. Eng.*, 2018, **310**, 1–7.

17 L. Tellez, J. Rubio, F. Rubio, E. Morales and J. L. Oteo, Synthesis of Inorganic-Organic Hybrid Materials from TEOS, TBT and PDMS, *J. Mater. Sci.*, 2003, **38**(8), 1773–1780.

18 X. Zhang, H. Ye, B. Xiao, L. Yan, H. Lv and B. Jiang, Sol–Gel Preparation of PDMS/Silica Hybrid Antireflective Coatings with Controlled Thickness and Durable Antireflective Performance, *J. Phys. Chem. C*, 2010, **114**(47), 19979–19983.

19 J. Lin and K. Baerner, Tunable Photoluminescence in Sol–Gel Derived Silica Xerogels, *Mater. Lett.*, 2000, **46**(2–3), 86–92.

20 J. D. Mackenzie, Q. Huang and T. Iwamoto, Mechanical Properties of Ormosils, *J. Sol-Gel Sci. Technol.*, 1996, **7**(3), 151–161.

21 C. F. Song, M. K. Lü, P. Yang, F. Gu, D. Xu and D. R. Yuan, A Potential Blue Photoluminescence Material: ZrO_2–SiO_2 Glasses, *Mater. Sci. Eng., B*, 2002, **94**(2–3), 181–185.

22 J. J. Velázquez, J. Mosa, G. Gorni, R. Balda, J. Fernandez, L. Pascual, A. Dwan and Y. Castro, Transparent SiO_2-GdF_3 Sol–Gel Nano-Glass Ceramics for Optical Applications, *J. Sol-Gel Sci. Technol.*, 2019, **89**, 322–332.

23 L. Zhang, Y. Yao, X. Ye and Q. Wu, Luminescence Behavior of Eu^{3+} in Polytitanasiloxane Solution, *J. Polym. Sci., Part B: Polym. Phys.*, 2006, **44**, 1357–1363.

24 S. Okuzaki, K. Okude and T. Ohishi, Photoluminescence Behavior of SiO_2 Prepared by Sol–Gel Processing, *J. Non-Cryst. Solids*, 2000, **265**(1), 61–67.

25 A. Sarkar and G. Gopal Khan, The formation and detection techniques of oxygen vacancies in Titanium oxide-based Nano-structures, *Nanoscale*, 2019, 1–32, DOI: 10.1039/C8NR09666J.

26 F. A. De Jesus, B. V. Santana, J. M. A. Caiut and V. H. V. Sarmento, Local Coordination, Influence on Synthesis and Luminescent Features of Eu^{3+} Ions in SiO_2-Poly(methyl methacrylate) Hybrid Materials, *Ind. Eng. Chem. Res.*, 2018, **57**(11), 3941–3949.

27 S. Kasturi and V. Sivakumar, Luminescence Properties of $La_2W_{2-x}Mo_xO_9$ (x = 0–2): Eu^{3+} Materials and Their Judd–Ofelt Analysis: Novel Red Line Emitting Phosphors for pcLEDs, *Mater. Chem. Front.*, 2017, **1**(3), 550–561.

28 S. Selvi, K. Marimuthu, N. Suriya Murthy and G. Muralidharan, Red Light Generation Through the Lead Boro-telluro-phosphate Glasses Activated by Eu^{3+} Ions, *J. Mol. Struct.*, 2016, **1119**, 276–285, DOI: 10.1016/j.molstruc.2016.04.073.

29 H. You and M. Nogami, Optical Properties and Local Structure of Eu^{3+} Ions in Sol–Gel TiO_2–SiO_2 Glasses, *J. Phys. Chem. B*, 2004, **108**(32), 12003–12008.

30 Y. Tian, B. Chen, R. Hua, J. Sun, L. Cheng, H. Zhong, *et al.*, Optical Transition, Electron-Phonon Coupling and Fluorescent Quenching of $La_2(MoO_4)_3$:Eu^{3+} phosphor, *J. Appl. Phys.*, 2011, **109**(5), 1–7.

31 M. A. Bizeto, V. R. L. Constantino and H. F. Brito, Luminescence properties of the layered niobate $KCa_2Nb_3O_{10}$ doped with Eu^{3+} and La^{3+} ions, *J. Alloys Compd.*, 2000, **311**, 159–168.

32 B. B. J. Basu and N. Vasantharajan, Temperature Dependence of the Luminescence Lifetime of a Europium Complex Immobilized in Different Polymer Matrices, *J. Lumin.*, 2008, **128**(10), 1701–1708.

33 J. M. M. Buarque, D. Manzani, S. L. Scarpari, M. Nalin, S. J. L. Ribeiro, J. Esbenshade, *et al.*, SiO_2–TiO_2 doped with Er^{3+}/Yb^{3+}/Eu^{3+} Photoluminescent Material: A Spectroscopy and Structural Study about Potential Application for Improvement of the Efficiency on Solar Cells, *Mater. Res. Bull.*, 2018, **107**, 295–307, DOI: 10.1016/j.materresbull.2018.07.007.

34 B. Julian, H. Beltrán, E. Cordoncillo, P. Escribano, B. Viana and C. Sanchez, Influence of the Matrix in the Optical Response of Organic-Inorganic Hybrid Materials Doped with Europium(III), *J. Sol-Gel Sci. Technol.*, 2003, **26**(1–3), 977–980.

35 S. K. Jose, S. Gopi, S. M. Simon, P. R. Mohan, C. Joseph, N. V. Unnikrishnan, *et al.*, Structural and Optical Characterization of Eu^{3+} Doped Polymer-Zirconia Composites, *J. Non-Cryst. Solids*, 2016, **452**, 245–252, DOI: 10.1016/j.jnoncrysol.2016.08.041.

36 L. Skuja, Optically Active Oxygen-Deficiency-Related Centers in Amorphous Silicon dioxide, *J. Non-Cryst. Solids*, 1998, **239**, 16–48.

37 T. Miyakawa and D. L. Phonon Sidebands, Multiphonon relaxation of Excited states, and phonon – assisted energy

transfer between ions in solids, *Phys. Rev. B: Solid State*, 1970, **1**(7), 2961–2969.

38 J. Dhanalakshmi, S. Iyyapushpam, S. T. Nishanthi, M. Malligavathy and D. P. Padiyan, Investigation of Oxygen Vacancies in Ce Coupled TiO_2 Nanocomposites by Raman and PL Spectra, *Adv. Nat. Sci.: Nanosci. Nanotechnol.*, 2017, **8**(1), aa5984, DOI: 10.1088/2043-6254/aa5984.

39 M. F. Best and R. A. Condrate, A Raman study of TiO_2–SiO_2 glasses prepared by sol–gel processes, *J. Mater. Sci. Lett.*, 1985, **4**, 994–998.

40 B. Karmakar, *Glass Nanocomposites*, Elsevier Inc., 2016, pp. 3–53, DOI: 10.1016/B978-0-323-39309-6.00001-8.

41 L. Marchese, E. Gianotti, V. Dellarocca, T. Maschmeyer, F. Rey, J. M. Thomas, *et al.*, Structure – functionality relationships of grafted Ti-MCM41 silicas. Spectroscopic and catalytic studies, *Phys. Chem. Chem. Phys.*, 1999, **1**, 585–592.

42 B. Deva Prasad Raju and C. Madhukar Reddy, Structural and Optical Investigations of Eu^{3+} Ions in Lead Containing Alkali Fluoroborate Glasses, *Opt. Mater.*, 2012, **34**(8), 1251–1260, DOI: 10.1016/j.optmat.2012.01.027.

43 W. Stambouli, H. Elhouichet, B. Gelloz and M. Férid, Optical and Spectroscopic Properties of Eu-Doped Tellurite Glasses and Glass Ceramics, *J. Lumin.*, 2013, **138**, 201–208.

44 B. Peng and T. Izumitani, The Fluorescence Properties of Eu^{3+} in Various Glasses and the Energy Transfer Between Eu^{3+} and Sm^{3+} in Borosilico-phosphate Glass, *Rev. Laser Eng.*, 1994, **22**(1), 16–27.

45 B. R. Judd, Optical Absorption Intensities of Rare-Earth Ions, *Phys. Rev.*, 1962, **127**(3), 750–761, DOI: 10.1103/PhysRev.127.750.

46 G. S. Ofelt, Intensities of Crystal Spectra of Rare-Earth Ions, *J. Chem. Phys.*, 1962, **37**(3), 511–520.

47 Y. Zheng, Y. Chen, C. Yang, Q. Wang, J. Lin and L. Zhang, Design of Europium doped SiO_2–TiO_2 Hybrids as Novel Luminescent Photocatalyst, *J. Lumin.*, 2012, **132**(7), 1639–1641.

48 C. Manjunath, M. S. Rudresha, B. M. Walsh, R. Hari Krishna, B. S. Panigrahi and B. M. Nagabhushana, Optical Absorption Intensity Analysis Using Judd–Ofelt Theory and Photoluminescence Investigation of Orange-Red Sr_2SiO_4:Sm^{3+} Nanopigments, *Dyes Pigm.*, 2018, **148**, 118–129.